TÉCNICO LISBOA

Hydrodynamic analysis of a dual-body Wave Energy Converter device with two different Power Take-off configurations

Julio Cesar de Souza Filho

Instituto Superior Técnico, Universidade de Lisboa, Portugal

ABSTRACT: The aim of the present research was to study the improvement of the efficiency of dual body wave energy converters by changing the configuration of the PTO installed. This was done by optimizing two different configurations for the WEC (PTO in between the floater and the submerged body, and PTO in between submerged body and sea bottom) to be installed in the region of Pico-Azores. The study is considered to be important as a higher efficiency means less cost to generate energy, being this one of the main barriers of the usage of WEC's nowadays. The analyzes begins with the modeling of the bodies of each WEC in NEMOH. This software allows the calculation of the hydrodynamical coefficients of the bodies (floaters and submerged bodies). With all the hydrodynamical coefficients calculated it was possible to create a dynamical model in frequency domain that optimizes and compares the maximum efficiency of the two configurations After that, previous researches that carried out similar calculations were found, this was done in order to validate the model. The model was validated by entering all the parameters equal to the ones in the researches and compare the outputs (hydrodynamical coefficients, absorbed power, efficiency and also sea spectrum creation). All outputs were found to be similar and so the model was considered to be validated. Finally, the presentation of the results was done. The comparison was made for three different combinations of bodies geometries (cylinder-sphere, cylinder-cylinder, and sphere-sphere, for the floater and submerged body respectively). The second configuration was considered more efficient, having an average improvement in the efficiency of 10.85%. It was also discovered that the second configuration is optimized for smaller bodies is compared to the first one.

1. Introduction

The world consumption of energy is rapidly increasing since the 1950's (due to different reasons, such as population, industrialization and urbanization growth) and the majority of research in the area shows this will continue in the next years.

The projection made by EIA (U.S. Energy Information Administration) also shows that the main primary energy source production will be renewable, such as wave energy.

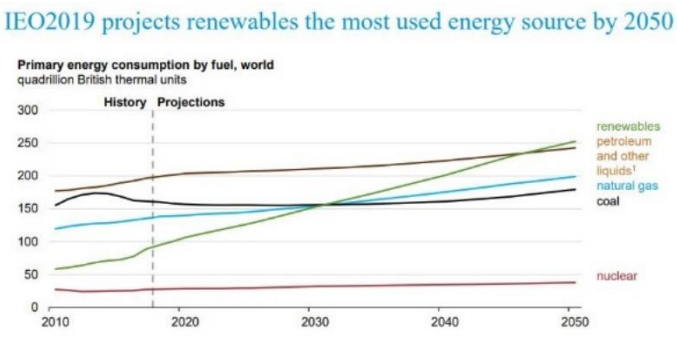

Figure 1:Projection about primary energy consumption in 2050

The exploration of wave energy started recently (R&D started around 1970's and demonstrations of wave energy converter devices around 1980's) so there is still a lot of development to be done in order to optimize its efficiency and lower the costs of installation and operation, being this the major issues when using wave energy converters nowadays.

Moreover, Mørk et al. (2010), has estimated that the global availability of gross power of wave energy is about 3.7 TW, while the installed capacity around the end of 2016 was only 12 MW, OES (2016). Annual Report 2016.

To understand the dimension of the power availability, it would represent 32412 TWh in one year (ignoring loses due to lack of perfect efficiency), and the world consumption of energy in 2019 was 173340 TWh, Ritchie (2017). Now it is possible to affirm that, besides the potential to represent near 20% of worlds consumption, wave energy is hugely underused (less than 1% of its potential). That means that any improve in the field could significantly increase the worlds power generation, something that will almost undeniably be one of the problems for the future years.

It is also important to remember the environmental effect of using wave energy instead of non-renewable ones. As it is renewable, it does not pollute the

environment as strongly as some traditional energy sources (as coal or oil for example), also it is not as dangerous to deal as nuclear energy.

The recent estimation made by OES (2017). International Vision for Ocean Energy Report 2017 shows that the ocean energy sector is expected to quickly grow in the next years, reaching a total of 300 GW by 2050 and so saving 500 million tons of CO2 emissions and creating approximately 680000 jobs.

In sum, it is possible to say now that there are several good reasons and needs to continue the studies in the field of wave energy exploration. The present research focused on solving one of the main problems with this source of energy, improving its efficiency, and that is of paramount importance, as improving the efficiency of a Wave Energy Converter means, in other worlds, reducing the cost to generate energy.

The reduction of the cost is one of the main challenges in the field today, as the technology to install it already exists.

There are multiple devices that are able to extract energy from the waves, called Wave Energy Converters (WECs), the present study focused on the optimization of a two-body point absorber to be installed in Pico-Azores using two different power take off systems (the first configuration consists of the PTO being installed between the two bodies, the second configuration consists of the PTO being installed between the submerged body and sea bottom).

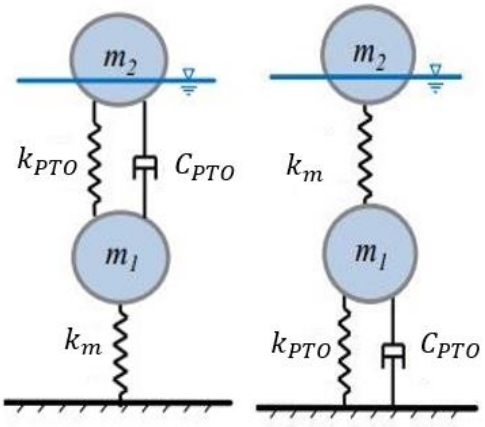

(a) *(b)*

Figure 2:(a) Dynamic model first configuration, (b) Dynamic model of Second Configuration

The main desire is to optimize both configurations varying it geometrical, PTO and mooring parameters in a range of values (more explanations about how it was done in further sections), and then prove that the second configuration is better than the first one in terms of harvesting energy efficiency.

2. Literature Review

A wave energy converter is a device that captures energy from the waves and converts it into electrical energy.

Normally, the wave energy is harvested by the movements of the device. There are several different types of WECs and therefore they can be classified into different groups.

One of the possible classifications is by the distance to the shoreline, studied by Cruz (2008); Falcão (2010); Guedes Soares et al (2012), classifying them into onshore, near shore and offshore.

Another one is the one used by The European Marine Energy Center LTD (EMEC) and also Guedes Soares et al (2012). In which the device is classified into 8 different types: attenuator, oscillating wave surge converter, oscillating water column, overtopping/terminator device, submerged pressure differential, bulge wave, rotating mass, point absorber and others.

2.1. Classification based on the distance to the shoreline

Figure 3 shows the different places that the WEC can be installed and the power availability in each of those places.

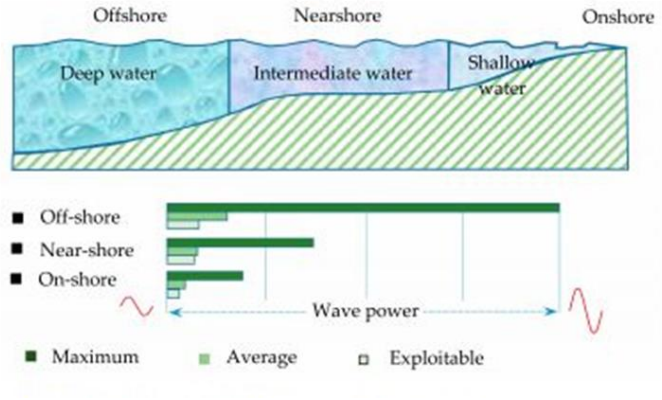

Figure 3: Classification based on the position of the WEC and energy available

Onshore WECs are usually fixed or embedded to the shoreline, this brings the advantage of easier and cheaper installation and maintenance. Although, in the shorelines the waves carry less energy and also some geometrical restriction maybe applied in order to preserve the landscape near the coast.

The near shore WECs are usually installed in water depths around 10m-25m and a distance around 500m from the shoreline. This kind of device has harder and more expensive installation and maintenance then the

onshore ones (however, it stills a lot easier and cheaper than the offshore ones) but it is exposed to waves carrying more energy.

The offshore devices are in areas far away from the shoreline and water depths over 40m (Deepwater). This kind of device usually is installed floating or near-surface and receives the most energy from the waves. Also, it allows the installations of a farm of devices due to the great availability of sea space. However, as they are receiving high energy waves they suffer with high structural loads on the device and on its mooring system and a higher risk of being damage by a storm.

2.2. Classification based on EMEC

Attenuator

An attenuator is a floating device which operates parallel to the dominant wave direction and effectively rides the waves. These devices capture energy from the relative motion of the two arms as the wave passes them.

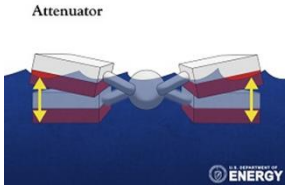

Figure 4:Attenuator WEC

Oscillating wave surge converters

An oscillating wave surge converters extract energy from wave surges and the movement of water particles within them. The arm oscillates as a pendulum mounted on a pivoted joint in response to the movement of water in the waves.

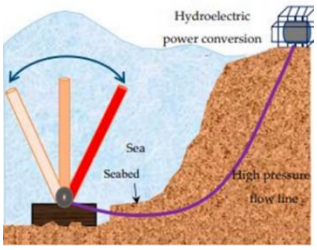

Figure 5:Oscillating Wave Surge Converter

Oscillating water column

An oscillating water column is a partially submerged, hollow structure. It is open to the sea below the water line, enclosing a column of air on top of a column of water. Waves cause the water column to rise and fall, which in turn compresses and decompresses the air column.

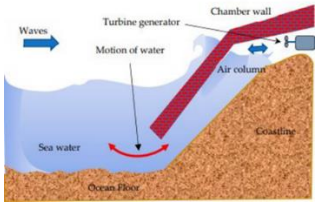

Figure 6:Oscillating Water Column

Overtopping/Terminator

Overtopping devices capture water as waves break into a storage reservoir. The water is then returned to the sea passing through a conventional low-head turbine which generates power. An overtopping device may use 'collectors' to concentrate the wave energy.

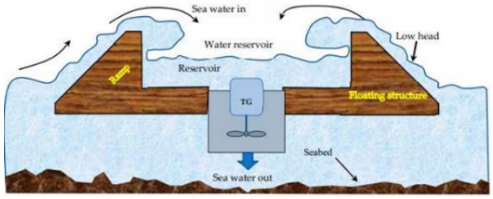

Figure 7:Overtopping/Terminator Device

Submerged pressure differential

Submerged pressure differential devices are typically located near shore and attached to the seabed. The motion of the waves causes the sea level to rise and fall above the device, inducing a pressure differential in the device. The alternating pressure pumps fluid through a system to generate electricity.

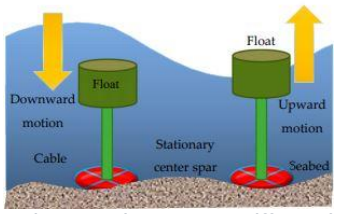

Figure 8:Submerged Pressure Differential Device

Bulge wave

Bulge wave technology consists of a rubber tube filled with water, moored to the seabed heading into the waves. The water enters through the stern and the passing wave causes pressure variations along the length of the tube, creating a 'bulge'. As the bulge travels through the tube it grows, gathering energy which can be used to drive a standard low-head turbine located at the bow, where the water returns to the sea.

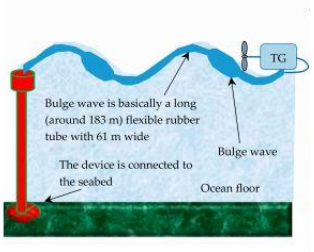

Figure 9:Bulge Wave Device

Rotating mass

Two forms of rotation are used to capture energy by the movement of the device heaving and swaying in the waves. This motion drives either an eccentric weight or a gyroscope causes precession. In both cases the movement is attached to an electric generator inside the device.

Rotating mass wave power device operates the motion of wave to roll a physical heavy object (mass) that produces mechanical energy. The rotating mass receives mechanical power from the oceanic wave and supplies it to the electrical generator

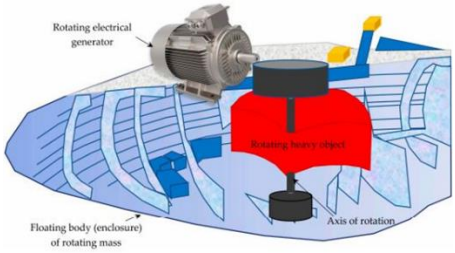

Figure 10:Rotating Mass Device

Point Absorber

As this is the WEC studied in the present study more considerations about it were made.

A point absorber is a floating structure which absorbs energy from all directions through its movements at/near the water surface. It converts the motion of the buoyant top relative to the base into electrical power.

The main consideration about point absorbers is that it harvests energy just by the heave movement of the wave, it is considered to be fixed in all other degrees of freedom.

A point absorber can be composed by one or more bodies. For instance, in the present research a two bodies point absorber is considered, but there are point absorber with one body, three or so on. Al Shami et al (2019), for example, presented point absorbers composed of two, three, four and five bodies and compared them.

A point absorber is usually composed by a number of bodies (the buoys), a mooring system, that can be developed in several different ways according to the design proprieties and a power take-off system (PTO), that may take a number of forms, depending on the configuration of displacers/reactors.

In the present study two different locations for the PTO were studied, the PTO being installed between the two bodies and the PTO being installed between the submerged body and sea bottom).

These components (PTO and mooring) are usually optimized in accordance with the place that the wave energy converter is going to be installed, there are several different methods to optimize them.

Besides being optimized, these components can be also put under some control method, that will change its proprieties in accordance with sea conditions to maximize the energy generated.

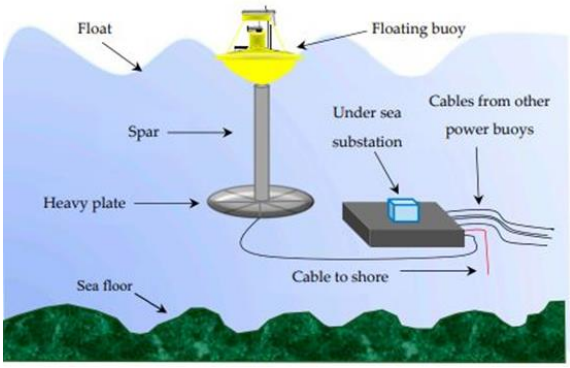

Figure 11:Point Absorber Device

Other

This covers those devices with a unique and quite different design to the more well-established types of technology or if information on the device's characteristics could not be determined. For example, the Wave Rotor, is a form of turbine turned directly by the waves. Flexible structures have also been suggested, whereby a structure that changes shape/volume is part of the power take-off system.

3. Mathematical Model

The goal of these section is to describe a mathematical model (using both a BEM solver software, NEMOH, and a code created in MatLab) that allows the calculation of the efficiency/Power Absorbed, both in regular and irregular waves, of the two models/configurations of the WEC's considered (the first configuration consists of the PTO being installed between the two bodies, the second configuration consists of the PTO being installed between the submerged body and sea bottom).

With this model correctly developed it is possible to optimize the efficiency based on the variation of the WEC's parameters. So, it is vital that this model is as reliable as possible. The main guarantee of the reliability of the model is obtained by, after the development of the model, carrying out a process of validation of all the results obtained that were already similarly calculated by other papers and researchers.

In the present study the analyzes was carried out using a frequency domain analyzes, like the ones proposed by Al Shamiet al (2018); Liang and Zuo (2016); Al Shami et al (2019).

The description of the model will be done in parts, firstly by the description of the BEM solver NEMOH, then the dynamic model of both configurations and finally the calculations of efficiency and power absorbed for both regular and irregular waves.

3.1. BEM solver NEMOH

In order to create the dynamic model in frequency domain and carry out the necessary calculations it is necessary to calculate the frequency-dependent hydrodynamic parameters of the two bodies (added mass, radiation damping, and wave forces).

There are some programs specialized in this calculation, for example WAMIT and NEMOH, a comparison between the two of them was made by Penalba et al (2017) showing good agreement between them. NEMOH was the one chosen.

NEMOH is a program based on the linear and second-order potential theory. To proceed with the calculations the velocity potential and fluid pressure on the submerged surfaces of the bodies are determined with the boundary element method.

Finally, the program solves the equations and from this solution obtains the hydrodynamic parameters.

NEMOH require some inputs in order to work and proceed with the calculations, a mesh file with the discretization of the panels for both bodies, conditions of the sea (like water depth, wave height, distance between the bodies and draft of the floating buoy) and values assumed for gravity and ρ.

In order to proper perform the calculations NEMOH makes some assumption, as it is described by the developer of the code in Babarit and Delhommeau (2015). The assumptions are inviscid fluid, incompressible and irrotational flow (which means the velocity derivates from a velocity potential and the pressure is obtained from Bernoulli formula).

The governing equation that is solved is Laplace equation.

$$\nabla^2\varphi = 0 \tag{1}$$

Where φ is the corresponding potential function of the fluid flow, the boundary conditions can be described by (being M the point considered for the calculations):

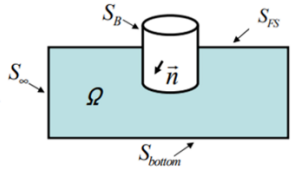

Figure 12:Model of the buoy to explain NEMOH equations

$$\Delta\phi = 0;\ \mathrm{M} \in \Omega \tag{2}$$

$$\frac{\partial\phi}{\partial n} = \vec{V}\vec{n};\ \mathrm{M} \in S_B \tag{3}$$

$$\frac{\partial\phi}{\partial n} = 0;\ \mathrm{M} \in S_{bottom} \tag{4}$$

$$\frac{\partial n}{\partial t} + \vec{\nabla}n\,\vec{\nabla}\phi = 0;\ \mathrm{M} \in S_{FS} \tag{5}$$

$$\frac{\partial\phi}{\partial t} + gn + 0.5\left(\vec{\nabla}\phi\right)^2 = 0;\ \mathrm{M} \in S_{FS} \tag{6}$$

Using all the boundaries conditions it is possible then to solve the Laplace equation and so solve the problem for the hydrodynamical coefficients.

3.2. Dynamic Model of First Configuration

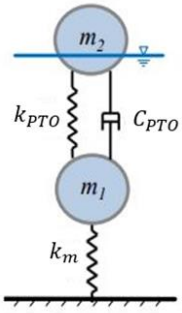

Figure 13:Dynamic Model First Configuration

Firstly, it is important to clarify that the movement of the dual body WEC is restricted to heave and the two bodies are coupled due to the PTO forces, so the system has two degrees of freedom (heave movement for the buoy and heave movement for the submerged body).

The model is based on the linear wave theory, meaning small wave amplitudes and small body motions were considered. As described before, the analyzes was developed in frequency domain.

In order to create the model, Newton's second law was applied for both bodies.

$$M\ddot{x} = \sum F_{external} \tag{7}$$

For the first body, also considering the interaction between the two bodies, equation (7) becomes:

$$\begin{aligned} m_1\ddot{x}_1 + A_{11}\ddot{x}_1 + A_{12}\ddot{x}_2 + b_{11}\dot{x}_1 + b_{12}\dot{x}_2 \\ + b_{visc1}\dot{x}_1 + c_{pto}(\dot{x}_1 - \dot{x}_2) \\ + k_{pto}(x_1 - x_2) + k_s x_1 = F_{e1} \end{aligned} \tag{8}$$

In order to use the frequency domain instead of time domain the excitation wave is assumed to be a regular sinusoid and the buoy displacement assumed harmonic. Then it is possible to consider, as in Al Shamiet al (2018); Liang and Zuo (2016); Al Shami et al

(2019); Cheng et al. (2014), that the exciting force and buoy displacement can be expressed as:

$$F_{e1} = F_1 e^{i\omega t} \quad (9)$$

And

$$x_1 = X_1 e^{i\omega t} \quad (10)$$

Substituting equations (9) and (10) in equation (8) it becomes:

$$\begin{aligned} -\omega^2(m_1 + A_{11})X_1 - \omega^2 A_{12}X_2 + i\omega b_{11}X_1 \\ + i\omega b_{12}X_2 + i\omega b_{visc1}X_1 \\ + i\omega c_{pto}(X_1 - X_2) \\ + k_{pto}(X_1 - X_2) + k_s X_1 \\ = F_1 \end{aligned} \quad (11)$$

Analogously, the equation for the submerged body became:

$$\begin{aligned} -\omega^2(m_2 + A_{22})X_2 - \omega^2 A_{21}X_1 + i\omega b_{22}X_2 \\ + i\omega b_{21}X_1 + i\omega b_{visc2}X_2 \\ + i\omega c_{pto}(X_2 - X_1) \\ + k_{pto}(X_2 - X_1) - k_m X_2 \\ = F_2 \end{aligned} \quad (12)$$

It is possible now to model the system as:

$$Z(i\omega) = -\omega^2 M + i\omega C + K \quad (13)$$

Where Z is the impedance matrix and can be written as:

$$Z(i\omega) = \begin{bmatrix} Z_{11} & Z_{12} \\ Z_{21} & Z_{22} \end{bmatrix} \quad (14)$$

With:

$$\begin{aligned} Z_{11} = -\omega^2(m_1 + A_{11}) + i\omega(b_{11} + b_{visc1} \\ + c_{pto}) + k_s + k_{pto} \end{aligned} \quad (15)$$

$$Z_{12} = -\omega^2 A_{12} + i\omega(b_{12} - c_{pto}) - k_{pto} \quad (16)$$

$$Z_{21} = -\omega^2 A_{21} + i\omega(b_{21} - c_{pto}) - k_{pto} \quad (17)$$

$$\begin{aligned} Z_{22} = -\omega^2(m_2 + A_{22}) + i\omega(b_{22} + b_{visc2} \\ + c_{pto}) + k_{pto} - k_m \end{aligned} \quad (18)$$

The solution for the equations (15), (16), (17) and (18) can now be written as:

$$X = Z(i\omega)^{-1} F \quad (19)$$

3.3. Dynamic Model of Second Configuration

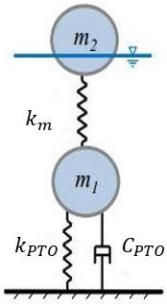

Figure 14:Dynamic Model Second Configuration

The development of the dynamic model of the second geometry is analogous to the first one. The variable k_m in this case is the connection stiffness between the two floaters, this variable was created like this to provide a fair comparison between the two configurations, as this way both configurations have the same number of variables in the model.

The equations of motion for this configuration became:

For the first body:

$$\begin{aligned} -\omega^2(m_1 + A_{11})X_1 - \omega^2 A_{12}X_2 + i\omega b_{11}X_1 \\ + i\omega b_{12}X_2 + i\omega b_{visc1}X_1 \\ + k_m(X_1 - X_2) + k_s X_1 = F_1 \end{aligned} \quad (20)$$

For the second body:

$$\begin{aligned} -\omega^2(m_2 + A_{22})X_2 - \omega^2 A_{21}X_1 + i\omega b_{22}X_2 \\ + i\omega b_{21}X_1 + i\omega b_{visc2}X_2 \\ - i\omega c_{pto}X_2 + k_m(X_2 - X_1) \\ - k_{pto}X_2 = F_2 \end{aligned} \quad (21)$$

Then, the impedance matrix became:

$$\begin{aligned} Z_{11} = -\omega^2(m_1 + A_{11}) + i\omega(b_{11} + b_{visc1}) \\ + k_s + k_m \end{aligned} \quad (22)$$

$$Z_{12} = -\omega^2 A_{12} + i\omega(b_{12}) - k_m \quad (23)$$

$$Z_{21} = -\omega^2 A_{21} + i\omega(b_{21}) - k_m \quad (24)$$

$$\begin{aligned} Z_{22} = -\omega^2(m_2 + A_{22}) + i\omega(b_{22} + b_{visc2} \\ - c_{pto}) - k_{pto} + k_m \end{aligned} \quad (25)$$

And finally, the solution is now calculated the same way of the first geometry:

$$X = Z(i\omega)^{-1} F \quad (26)$$

3.4. Power and Efficiency for Regular Wave

The efficiency for regular waves is defined as the ratio between the power absorbed by the WEC and the maximum power available to be absorbed in the income wave. The calculation is carried out for each different frequency of incoming waves.

$$\eta(\omega) = \frac{P_{avg}(\omega)}{P_{max\_wave}(\omega)} \quad (27)$$

The calculation of the power absorbed for each frequency of income wave can be calculated as in Al Sham et al (2018); Liang and Zuo (2016); Al Shami et al (2019); Cheng et al. (2015). It is important to notice that they are different for the first and second geometry, as the PTO (which generates the power) is placed in different places. For the first geometry it generates power in relation to the relative motion between the two bodies, for the second, in relation to the absolute motion of the second body.

For the first configuration:

$$P_{avg}(\omega) = \frac{1}{T}\int_0^T c_{pto}(\dot{x}_1 - \dot{x}_2)dt = 0.5\omega^2 c_{pto}\,abs(X_1 - X_2) \quad (28)$$

For the second configuration:

$$P_{avg}(\omega) = \frac{1}{T}\int_0^T c_{pto}(\dot{x}_2)dt = 0.5\omega^2 c_{pto}\,abs(X_2) \quad (29)$$

And the maximum power available in the wave to be absorbed by the WEC according to Dean and Darimple, (2010) can be calculated as the total energy per wave per unit width times the group velocity.

$$P_{max\_wave}(\omega) = Ec_g(\omega) \quad (30)$$

Where:

$$E = 0.5\rho g H^2 L \quad (31)$$

And

$$c_g(\omega) = 0.5\frac{\omega}{\kappa}\left(1 + (2\kappa(\omega)D_{epth})/(\sinh 2\kappa(\omega)D_{epth})\right) \quad (32)$$

3.5. Power and Efficiency for Irregular Waves

The calculation for irregular waves depends on the sea state of the place where the WEC is installed.

The parameters taken into considerations are the significant wave high (H_s) and energy wave period (T_e), more considerations about the Sea State are about to be made in the next section. The efficiency can then be calculated as described in Liang and Zuo (2016); Cheng et al. (2015).

$$\eta = \frac{P_{avg\_irr}}{P_{max\_wave\_irr}} \quad (33)$$

It is possible to notice that unlike in regular waves, the final efficiency is one number independent on the income wave frequency.

The calculation of absorbed and available power in irregular waves depends on the constructions of a sea spectra. The one chosen in this model was Pierson-Moskowitz spectra:

$$S(\omega) = 526H_s^2T_e^{-4}\omega^{-5}e^{-1054T_e^{-4}\omega^{-4}} \quad (34)$$

Now, both the absorbed and available power can be written as:

$$P_{irr} = \int_0^\infty P_{reg}(\omega)\,S(\omega)d\omega \cong \sum P_{reg}(\omega)\,S(\omega)\Delta\omega \quad (35)$$

3.6. Sea State

The place considered for the WEC to be installed is Pico-Azores. The states of the sea were found in Matos et al (2015). The study modeled the Sea State in Pico and the results found can be seen in Figure 15.

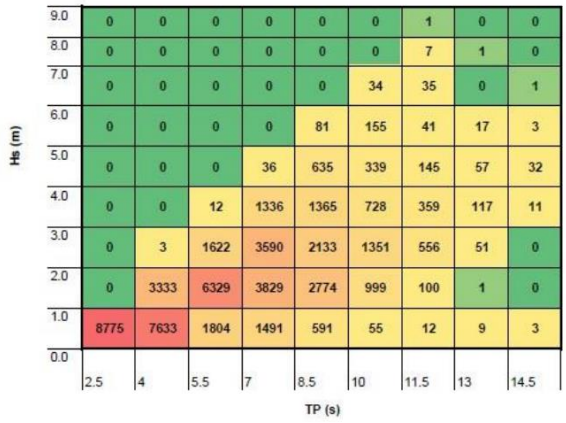

Figure 15:Description of Sea State Pico-Azores

The values seen in Figure 13 are the occurrence of each Sea State. So, dividing all of the cells by the total amount of occurrences registered it is possible to reach a percentage of each sea state.

With occurrence of each Sea State, the total spectrum is now the sum of all the spectrum of each sea state times its percentage of occurrence.

$$S(\omega) = \sum S_{SeaState}(\omega) * Occurence \quad (36)$$

4. Method of Optimization and code development

The optimization process is one of the main goals of this thesis, as this is the part responsible for guaranteeing that the best efficiency possible is reached, resulting in less cost to produce energy in a determined area.

Firstly, three different combinations of geometrical shapes were defined to be analyzed (cylinder-sphere, cylinder-cylinder, sphere-sphere for the floater and the submerged body respectively).

All the three combinations were analyzed for both the first configuration (PTO between the two bodies) and second configuration (PTO between submerged body and sea bottom)

The process described in the next lines was caried out for all the three configurations combined with both first and second configurations of the PTO, so it was carried out six times.

For example, the process can be carried out for the case of cylinder-sphere using the first configuration of the PTO, cylinder-sphere using the second configuration of the PTO, cylinder-cylinder using the first configuration of the PTO and so on.

The process consists of the creation of a loop in MatLab involving both the NEMOH software and codes created to perform the dynamical analyzes and optimization of the system (resulting in the calculation of absorbed power and efficiency).

First, the shape of the bodies being analyzed are defined (for example cylinder-sphere). Then, different mesh geometries are created in NEMOH (as much as the operator decides to input, as more geometries are set more computational time to run the program is needed) and the hydrodynamical coefficients outputted are stored in a '. MAT' file.

The meaning of this different meshes created is to set different sizes of the bodies to be analyzed, so, for example, it can be analyzed for the case cylinder-sphere (using the first PTO configuration) for different sizes of the cylinder combined with different sizes of the sphere (each one of these combinations generating a different mesh file in NEMOH).

So, for example one of this meshes could contain data about a cylinder-sphere WEC with a cylinder with 2 meters radius and 1 meter draft combined with a sphere with 2 meter radius, another one of this meshes could contain a cylinder with 1 meter radius and 0.5 meter of draft combined with a sphere with 1 meter radius, and so on (as many as the operator decides to set).

Then, a range of a range of values of PTO and mooring parameters (c_{pto}, K_{pto}, K_m) are defined and will be used to optimize the efficiency with the meshes created.

After, the loop proceeds to the calculation of efficiency and power absorbed (following the model described in this chapter) for all the different meshes (different combinations of bodies sizes) combined with all the different parameters (c_{pto}, K_{pto}, K_m).

Finally, the code points which is the best geometrical configuration and mooring and PTO parameters (c_{pto}, K_{pto}, K_m) that reached the maximum efficiency for the case analyzed.

For example, if the case been analyzed was cylinder-sphere using the first configuration of the PTO, the code would, in this stage, point which combination of mesh (sizes of the buoy and the submerged body) and mooring and PTO parameters (c_{pto}, K_{pto}, K_m) generated the maximum efficiency, being this the optimum case.

In short, the goal is to obtain the combination of parameters that generates the highest possible efficiency in irregular waves for one of the geometrical configurations (being this the highest possible efficiency for all the configurations inputted).

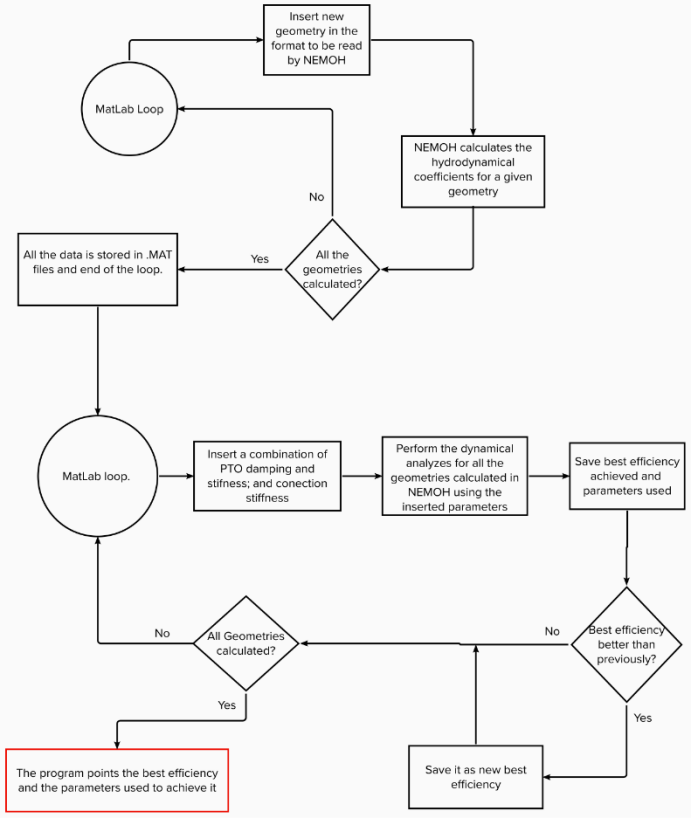

Figure 16:Workflow of the optimization method

5. Validation

The validation of the results was done in four parts. The objective of each of these parts is to compare the obtained values with the ones from existing papers.

Firstly, a single body wave energy converter was modeled using the exact same dimensions and parameters of one of the devices modeled in Ruezga (2019), the parameters compared in this case were all the hydrodynamical coefficients, the absorbed power and the RAO.

Secondly, a two-body wave energy converter was modeled following the same dimensions and parameters of the model in Al Shami et al (2019) the parameters compared were the hydrodynamical coefficients for both bodies and the absorbed power.

Then, the validation for irregular waves was carried out following the same structure and sea conditions presented in Engström et al (2009), the comparison made here was with the captured width radio presented in the paper and the one calculated.

Finally, the Spectrum of the Sea State considered was compared with the one described in Falcão et al (2002), as they are both modeling the same place (Pico-Azores) and so they should return the same value.

All comparisons ended up showing similar values between the obtained results and the papers, however, due to the lack of space just the validation of the two body wave energy converter is presented here.

5.1. Dual Body Wave Energy Converter

The structure considered is a cylindrical buoy and a sphere submerged body to compose the dual body wave energy converter with a PTO system in located in between the two bodies. The dynamical simplified model considered is shown in Figure 15.

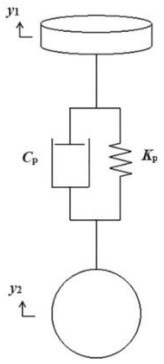

Figure 17:Dynamic Model of the WEC Considered

The analysis was carried considering 40 frequencies in a range from 0.05 rad/s to 3 rad/s and the parameters/dimensions of the analysis were the same as Al Shami et al (2019).

The mesh of the structure was done using the pre-processor of NEMOH. Two bodies were meshed and after the analyses was done using both of the meshes. The buoy was modeled using 686 panels and 2744 nodes. The submerged body was modeled using 980 panels and 3920 nodes.

Then, using the main processor and solver of NEMOH, the hydrodynamic coefficients were obtained for both buoy and submerged body and compared with the ones obtained in Al Shami et al (2019).

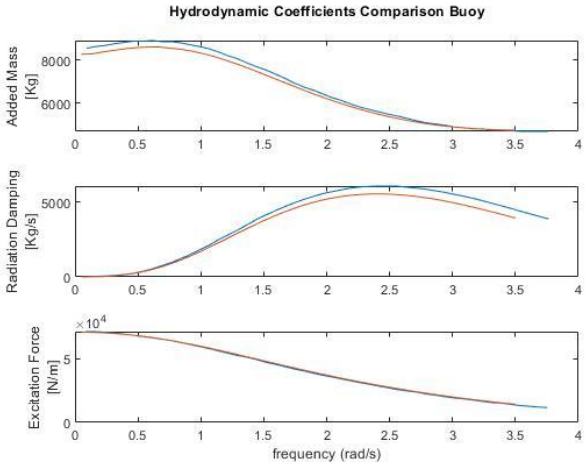

Figure 18:Hydrodynamic Coefficients Comparison for the Buoy for Validation of Dual Body WEC

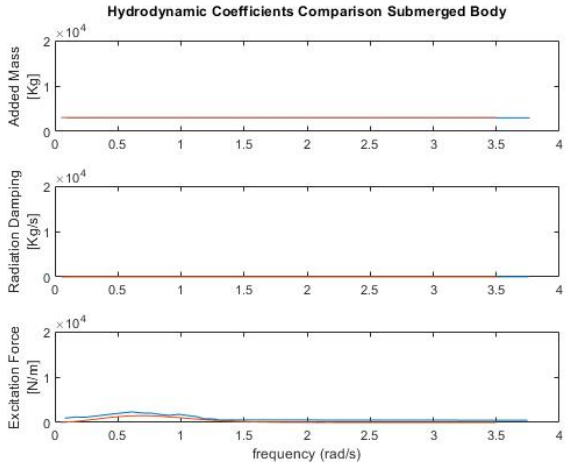

Figure 19:Hydrodynamic Coefficients Comparison for the Submerged Body for Validation of Dual Body WEC

In the possession of the hydrodynamic coefficients the calculations of the absorbed power were carried out and compared with the values obtained in Al Shami et al (2019).

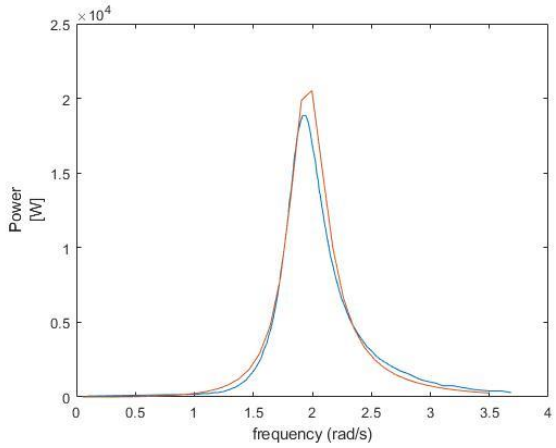

Figure 20:Average Absorbed Power Comparison for Validation of Dual Body WEC

6. Results

As said before, the Optimization Process was carried out for 3 different combinations of bodies (cylinder-sphere, cylinder-cylinder, sphere-sphere for the floater and the submerged body respectively). For each one of these combinations the analyzes for both configurations were carried out.

This process follows all the steps already better described and properly explained in the section Method of Optimization.

The range of values used for the parameters (c_{pto}, K_{pto}, K_m) and body sizes chosen were defined by looking at already existing papers and seeing which values are commonly used in these kinds of wave energy converters.

Due to the lack of space available, just an analyzes of all the efficiencies obtained was carried out. It was proven in the end that the second configuration is indeed more efficient than the first one in all the cases tested in the present thesis.

To simplify computational time required to perform the calculations all cylinders were modeled in NEMOH using 686 panels and 2744 nodes and all the spheres using 980 panels and 3920 nodes.

6.1. Discussion

As it can be seen in Table 31 all the efficiencies for the second configuration of the PTO optimized are higher than the first configuration. This means that it costs less money to generate energy in Pico-Azores using the second configuration (PTO between submerged body and sea bottom) instead of the first one (PTO between buoy and submerged body).

Table 1: Comparison of Optimal Design for all Geometrical Configurations (Cylinder-Sphere, Cylinder-Cylinder, Sphere-Sphere)

	First Configuration Optimized bodies	Second Configuration Optimized bodies
Geometrical Configuration	**Cylinder-Sphere**	
Buoy Radius [m]	2.5	1
Buoy Draft [m]	1	0.5
Submerged Body Radius [m]	3	1
Absorbed Power Irregular Waves [W]	1.26E+04	5.91E+03
Efficiency Irregular Waves	47.07%	55.43%
Geometrical Configuration	**Cylinder-Cylinder**	
Buoy Radius [m]	2.5	2.5
Buoy Draft [m]	2	1
Submerged Body Radius [m]	4	2.5
Submerged Body Heigth [m]	2.5	2
Absorbed Power Irregular Waves [W]	1.46E+04	1.86E+04
Efficiency Irregular Waves	54.86%	65.67%
Geometrical Configuration	**Sphere-Sphere**	
Buoy Radius [m]	2	2
Submerged Body Radius [m]	3	1
Absorbed Power Irregular Waves [W]	9.96E+03	1.28E+04
Efficiency Irregular Waves	46.67%	60.06%

The wave energy converter that reached the best efficiency was the cylinder-cylinder for both the first and the second configuration of the PTO. However, the second most efficient was the sphere-sphere, for the case of second PTO configuration, and cylinder-sphere for the case of first PTO configuration.

Also, it is possible to see that the second configuration of the PTO is optimized always for smaller bodies (both floater and submerged body, exception made for the case of cylinder-cylinder in which the size of the buoy is the same) in comparison with the first configuration, this is even more noticed in the case of the submerged body.

For the case cylinder-sphere, the size of the submerged sphere goes from 3 meters radius (first configuration of the PTO) to 1 meter (second configuration of the PTO).

For cylinder-cylinder it goes from 4 meters of radius and 2.5 meters of height (for the first PTO configuration) to 2.5 meters radius and 2 meters height (second configuration of the PTO).

For the case sphere-sphere it goes from 3 meters radius (for the first PTO configuration) to 1 meter (for the second PTO configuration).

Now, analyzing all the optimized data together, it is possible to notice that the first configuration of the PTO produced an average efficiency of 49.53%, while the second configuration of the PTO produced an average efficiency of 60.39%.

That means that using the second configurations instead of the first one generates an average improvement in the efficiency of the optimized data of 10.85%.

This means that the second configuration is indeed more efficient than the first one for all the cases analyzes. This final conclusion proofs the starting objective of the present thesis previously described.

7. References

Al Shami, E., Wang, X. and Ji, X., 2019. A study of the effects of increasing the degrees of freedom of a point-absorber wave energy converter on its harvesting performance. Mechanical Systems and Signal Processing, 133, p.106281.

Al Shami, E., Wang, X., Zhang, R. and Zuo, L., 2019. A parameter study and optimization of two body wave energy converters. Renewable energy, 131, pp.1-13.

Babarit, A. and G. Delhommeau (2015). "Theoretical and numerical aspects of the open source BEM solver NEMOH." 11th European Wave and Tidal Energy Conference (EWTEC2015).

Cheng, Z., Yang, J., Hu, Z. and Xiao, L., 2014. Frequency/time domain modeling of a direct drive point absorber wave energy converter. Science China Physics, Mechanics and Astronomy, 57(2), pp.311-320.

Cruz J (2008) Ocean Wave Energy: current status and future perspectives. Springer, Heidelberg p. 423.

Engström, J., Eriksson, M., Isberg, J. and Leijon, M., 2009. Wave energy converter with enhanced amplitude response at frequencies coinciding with Swedish west coast sea states by use of a supplementary submerged body. Journal of Applied Physics, 106(6), p.064512.

Falcão, A.F. and Rodrigues, R.J.A., 2002. Stochastic modelling of OWC wave power plant performance. Applied Ocean Research, 24(2), pp.59-71.

Falcão A. F. O. (2010) Wave Energy Utilization: A Review of the technologies. Renewable and Sustainable Energy Reviews, Volume 14, Issue 3, 2010, p. 899-918

Guedes Soares, C., Bhattacharjee, J., Tello, M. and Pietra, L., 2012. Review and classification of wave energy converters. Maritime Engineering and Technology. London: Taylor & Francis Group, pp.585-594

Liang, C. and Zuo, L., 2016, September. On the dynamics and design of a two-body wave energy converter. In Journal of Physics: Conference Series (Vol. 744, No. 1, p. 012074). IOP Publishing.

Matos, A., Madeira, F., Fortes, C.J.E.M., Didier, E., Poseiro, P. and Jacob, J., 2015. Wave energy at Azores islands. Proc., SCACR.

Mørk, G., et al. (2010). Assessing the Global Wave Energy Potential. ASME 2010 29th International Conference on Ocean, Offshore and Arctic Engineering.

OES (2016). Annual Report 2016. Available at: https://report2016.ocean-energy-systems.org (Accessed: 9 January 2021).

OES (2017). International Vision for Ocean Energy Report 2017. Available at: https://testahemsidaz2.files.wordpress.com/2017/03/oes-international-vision.pdf (Accessed: 9 January 2021).

Penalba, M., Kelly, T. and Ringwood, J., 2017. Using NEMOH for modelling wave energy converters: A comparative study with WAMIT.

Rezanejad, K., Guedes Soares, C., (2018) Enhancing the primary efficiency of an oscillating water column wave energy converter based on a dual-mass system analogy, Renewable Energy, Volume 123, 2018, Pages 730-747

Ruezga, A., 2019. Buoy Analysis in a Point-Absorber Wave Energy Converter. IEEE Journal of Oceanic Engineering, 45(2), pp.472-479.

Walton, R., 2019. Global electricity consumption to rise 79 percent higher by 2050, EIA says | Power Engineering. [online] Power Engineering. Available at: <https://www.power-eng.com/renewables/global-electricity-consumption-to-rise-79-percent-higher-by-2050-eia-says/> [Accessed 7 June 2020].

Zhao, X.L., Ning, D.Z., Zou, Q.P., Qiao, D.S. and Cai, S.Q., 2019. Hybrid floating breakwater-WEC system: A review. *Ocean Engineering*, *186*, p.106126.